

PAPER

# Polar-antipolar transition and weak ferromagnetism in Mn-doped $\text{Bi}_{0.86}\text{La}_{0.14}\text{FeO}_3$

To cite this article: V A Khomchenko *et al* 2018 *J. Phys. D: Appl. Phys.* **51** 165001

View the [article online](#) for updates and enhancements.

## Related content

- [Structural defects as a factor controlling the magnetic properties of pure and Ti-doped  \$\text{Bi}\_{1-x}\text{Ca}\_x\text{FeO}\_{3/2}\$  multiferroics](#)  
V A Khomchenko and J A Paixão
- [Composition- and temperature-driven structural transitions in  \$\text{Bi}\_{1-x}\text{Ca}\_x\text{FeO}\_3\$  multiferroics: a neutron diffraction study](#)  
V A Khomchenko, I O Troyanchuk, D M Többens *et al.*
- [Effect of Mn substitution on crystal structure and magnetic properties of  \$\text{Bi}\_{1-x}\text{Pr}\_x\text{FeO}\_3\$  multiferroics](#)  
V A Khomchenko, I O Troyanchuk, M I Kovetskaya *et al.*



**IOP | ebooks™**

Bringing you innovative digital publishing with leading voices to create your essential collection of books in STEM research.

Start exploring the collection - download the first chapter of every title for free.

# Polar-antipolar transition and weak ferromagnetism in Mn-doped $\text{Bi}_{0.86}\text{La}_{0.14}\text{FeO}_3$

V A Khomchenko<sup>1</sup>, D V Karpinsky<sup>2,3</sup>, I O Troyanchuk<sup>2</sup>, V V Sikolenko<sup>4,5</sup>, D M Többens<sup>6</sup>, M S Ivanov<sup>1</sup>, M V Silibin<sup>3</sup>, R Rai<sup>7</sup> and J A Paixão<sup>1</sup>

<sup>1</sup> Department of Physics, CFisUC, University of Coimbra, P-3004-516 Coimbra, Portugal

<sup>2</sup> Scientific-Practical Materials Research Centre of NAS of Belarus, 220072 Minsk, Belarus

<sup>3</sup> National Research University of Electronic Technology ‘MIET’, 124498 Zelenograd, Moscow, Russia

<sup>4</sup> Joint Institute for Nuclear Research, 141980 Dubna, Russia

<sup>5</sup> REC ‘Functional Nanomaterials’, Immanuel Kant Baltic Federal University, 236041 Kaliningrad, Russia

<sup>6</sup> Helmholtz-Zentrum Berlin for Materials and Energy, D-14109 Berlin, Germany

<sup>7</sup> School of Physics and Materials Science, Shoolini University, 173212 Solan, India

E-mail: [uladzimir@fis.uc.pt](mailto:uladzimir@fis.uc.pt) (V A Khomchenko)

Received 19 January 2018, revised 1 March 2018

Accepted for publication 9 March 2018

Published 28 March 2018



CrossMark

## Abstract

Having been considered as a prime example of a room-temperature magnetoelectric multiferroic,  $\text{BiFeO}_3$  continues to attract much interest. Since functional properties of this material can be effectively influenced by chemical, electrical, magnetic, mechanical and thermal stimuli, it can serve as a model for the investigation of cross-coupling phenomena in solids. Special attention is currently paid to the study of chemical pressure-driven magneto-structural transformations. In this paper, we report on the effect of the Mn doping on the crystal structure and magnetic behavior of the  $\text{Bi}_{1-x}\text{La}_x\text{FeO}_3$  multiferroics near their polar-antipolar (antiferromagnetic-weak ferromagnetic) phase boundary. Synchrotron x-ray and neutron powder diffraction measurements of the  $\text{Bi}_{0.86}\text{La}_{0.14}\text{Fe}_{1-x}\text{Mn}_x\text{O}_3$  ( $x = 0.05, 0.1, 0.15$ ) compounds have been performed. The diffraction data suggest that the Mn substitution results in the suppression of the ferroelectric polarization and gives rise to the appearance of the antiferroelectric (generally,  $\text{PbZrO}_3$ -related) phase characteristic of the phase diagrams of the  $\text{Bi}_{1-x}\text{RE}_x\text{FeO}_3$  ( $\text{RE} = \text{rare-earth}$ ) systems. Depending on the Mn concentration (determining phase composition of the  $\text{Bi}_{0.86}\text{La}_{0.14}\text{Fe}_{1-x}\text{Mn}_x\text{O}_3$  samples at room temperature), either complete or partial revival of the polar phase can be observed with increasing temperature. Magnetic measurements of the samples indicate that the Mn doping affects the stability of the cycloidal antiferromagnetic order specific to the polar phase, thus resulting in the formation of a ferroelectric and weak ferromagnetic state.

Keywords:  $\text{BiFeO}_3$ , crystal structure, magnetic properties, multiferroics, spin-cycloid instability

(Some figures may appear in colour only in the online journal)

## 1. Introduction

Magnetoelectric multiferroics are known as materials of immense practical potential. Indeed, coupling between the ferroelectric and magnetic order parameters provides the

possibility to control the polarization with a magnetic field and magnetization with an electric field—the property opening new horizons for spintronics and information processing technologies [1, 2]. Since most of the known magnetic ferroelectrics have low transition temperatures, bismuth ferrite ( $\text{BiFeO}_3$ ) with

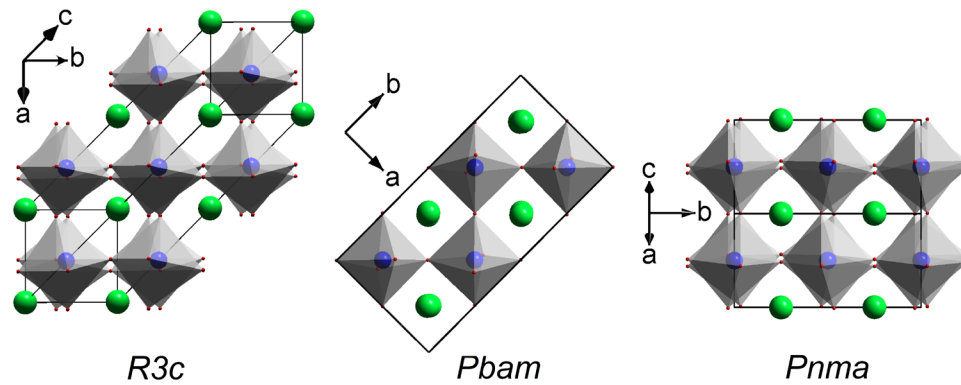


**Figure 1.** Schematic views of the unit cells for the polar rhombohedral (S. G.  $R3c$ ), antipolar orthorhombic (S. G.  $Pbam$ ) and nonpolar orthorhombic (S. G.  $Pnma$ ) phases along one of the three mutually perpendicular axes coincident with the  $\langle 100 \rangle_p$  directions of the parent cubic perovskite ( $ABO_3$ ) cell. The A-site (in green) and B-site (in blue) atoms are surrounded by oxygen (in red), thus forming the  $AO_{12}$  and  $BO_6$  (in grey) polyhedra.

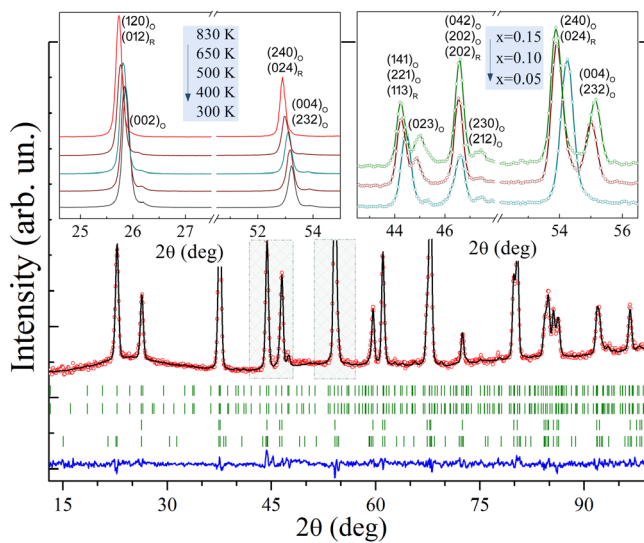


**Figure 2.** Experimental (red circles), calculated (black line) and difference (blue line) NPD patterns obtained for the  $Bi_{0.86}La_{0.14}Fe_{0.95}Mn_{0.05}O_3$  sample at room temperature. Tick marks indicate the positions of allowed nuclear and magnetic Bragg reflections for the antipolar orthorhombic (two upper rows) and polar rhombohedral (two lower rows) phases. The left inset shows experimental SPD patterns obtained for the  $x = 0.05$  compound at different temperatures (the data suggest the temperature-driven revival of the rhombohedral phase). The right inset shows experimental NPD patterns obtained for the  $Bi_{0.86}La_{0.14}Fe_{1-x}Mn_xO_3$  ( $x = 0.05, 0.1, 0.15$ ) compounds at room temperature (the data reflect the existence of composition-driven rhombohedral-to-orthorhombic (polar-antipolar) structural phase transformation).

the ferroelectric Curie temperature  $T_C \approx 1100$  K and antiferromagnetic Néel temperature  $T_N \approx 640$  K remains one of the most promising candidates for the room-temperature applications [3, 4]. The pure  $BiFeO_3$  is a perovskite-like material with a rhombohedral crystal lattice (space group (S. G.)  $R3c$ ) [5] and cycloidal magnetic structure [6] stable over a broad range of magnetic fields up to  $\sim 200$  kOe [7]. Due to the presence of the cycloidal modulation, magnetoelectric coupling arises from a quadratic term and remains weak [8]. When the cycloid is suppressed by a magnetic field, a small canting of the spin moments through the oxygen octahedra tilting gives rise to a weak magnetization, and a linear magnetoelectric coupling

appears [7, 9]. Both crystal and magnetic structures of  $BiFeO_3$  are strain sensitive and can thus be manipulated by applying epitaxial or chemical pressure [4, 9]. In particular, substitution of Bi by La induces the following sequence of phase transitions in the  $Bi_{1-x}La_xFeO_3$  series: the antiferromagnetic (AFM) and ferroelectric (FE) rhombohedral phase (S. G.  $R3c$ ) stable at  $x \leq 0.16$  transforms into the weak ferromagnetic (wFM) and antiferroelectric (AFE) orthorhombic phase (S. G.  $Pnam$  ( $Pbam$ , while applying the simplified structural model ignoring the presence of a small  $c^+/c^-$  component in the octahedral tilt pattern)) [10] stable in a narrow concentration range near  $x = 0.18$ ; the latter, in turn, transforms into the wFM/AFE phase with an incommensurately modulated structure (super-space group  $Imma(00\gamma)s00$ ) stable at  $0.19 \leq x \leq 0.3$ ; a further increase in the La content gives rise to the formation of the wFM nonferroelectric (NFE)  $GdFeO_3$ -type phase (S. G.  $Pnma$ ) [10, 11]. Similar composition-driven FE + AFM  $\rightarrow$  AFE + wFM  $\rightarrow$  NFE + wFM transformations can be observed in the  $Bi_{1-x}RE_xFeO_3$  ( $RE = Pr, Nd, Sm, Eu, Gd$ ) series [12, 13]. It has been recently shown that the partial chemical substitution of Fe with Mn can shift the boundaries of the magnetic and structural phases [14, 15] and can therefore be used to tune the multiferroic behavior of the  $Bi_{1-x}RE_xFeO_3$  perovskites. It is reasonable to suppose that the most pronounced effects associated with the Mn doping-driven magnetic and structural instabilities should be observed near a polar-antipolar phase boundary, where physical properties of the  $Bi_{1-x}RE_xFeO_3$  multiferroics are especially sensitive to such external stimuli as temperature, electric and magnetic fields, mechanical stress, etc [10, 16, 17]. In order to understand how Mn substitution affects the crystal structure and magnetic behavior of the polar antiferromagnets near the FE + AFM/AFE + wFM phase boundary, solid state synthesis and extensive diffraction/magnetometric study of the  $Bi_{0.86}La_{0.14}Fe_{1-x}Mn_xO_3$  ( $x \leq 0.15$ ) perovskites have been carried out.

## 2. Experimental

Polycrystalline samples of  $Bi_{0.86}La_{0.14}Fe_{1-x}Mn_xO_3$  ( $x = 0.05, 0.1, 0.15$ ) were prepared by a solid-state reaction method

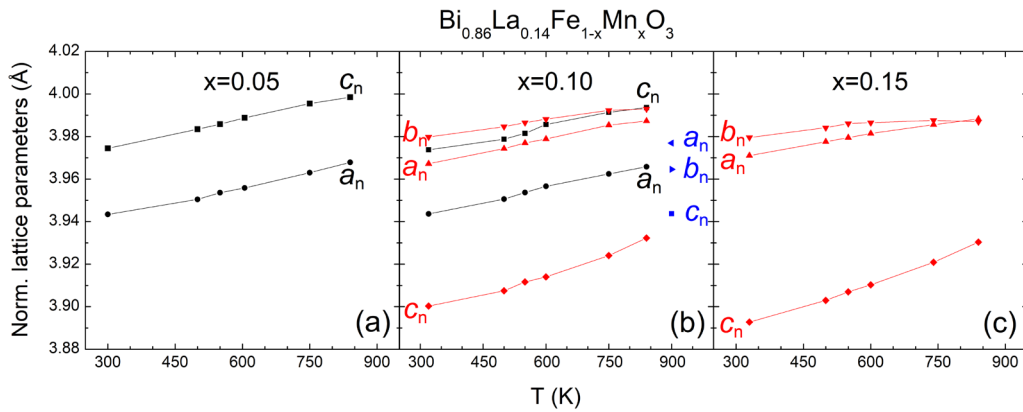


**Figure 3.** Normalized lattice parameters  $a_n$ ,  $b_n$  and  $c_n$  for the polar (black symbols), antipolar (red symbols) and nonpolar (blue symbols) phases of the  $\text{Bi}_{0.86}\text{La}_{0.14}\text{Fe}_{1-x}\text{Mn}_x\text{O}_3$  compounds as a function of temperature. Relationship between the normalized and unit cell parameters is given as follows:  $a_n = a/\sqrt{2}$ ,  $c_n = c/(2\sqrt{3})$  (polar rhombohedral phase, S. G.  $R3c$ ),  $a_n = a/\sqrt{2}$ ,  $b_n = b/(2\sqrt{2})$ ,  $c_n = c/2$  (antipolar orthorhombic phase, S. G.  $Pbam$ ),  $a_n = a/\sqrt{2}$ ,  $b_n = b/2$ ,  $c_n = c/\sqrt{2}$  (nonpolar orthorhombic phase, S. G.  $Pnma$ ). Temperature evolution of lattice parameters characterizing the antipolar phase of the  $x = 0.05$  compound cannot be reliably described due to a rapid suppression of this phase with increasing temperature.

using high-purity powders of  $\text{Bi}_2\text{O}_3$ ,  $\text{La}_2\text{O}_3$  (annealed at 1000 °C),  $\text{Fe}_2\text{O}_3$  and  $\text{Mn}_2\text{O}_3$  (Sigma-Aldrich,  $\geq 99\%$ ). The oxides were taken in a stoichiometric ratio, mixed in a planetary mill (Retsch PM 100) using isopropyl alcohol as a medium, and pressed into pellets. The samples were synthesized in air at 950 °C for 15 h followed by quenching to room temperature. X-ray diffraction (XRD) patterns were collected at room temperature using a Bruker D8 Advance diffractometer with  $\text{Cu } K_\alpha$  radiation. Synchrotron x-ray powder diffraction (SPD) study of the  $x = 0.05$  sample was performed at the German synchrotron light source BESSY-II (beam line KMC-2, wavelength 1.77 Å). Neutron powder diffraction (NPD) measurements of the  $x = 0.05$ , 0.1 and 0.15 samples were carried out at the Helmholtz-Zentrum Berlin for Materials and Energy (HZB) using the high-resolution diffractometer E9 with a wavelength of 1.7982 Å. The diffraction data were analyzed by the Rietveld method using the FullProf software package [18]. Magnetic measurements were performed with a cryogen-free Physical Properties Measurement System (PPMS DynaCool, Quantum Design).

### 3. Results and discussion

#### 3.1. Crystal structure as a function of chemical composition and temperature

X-ray diffraction measurements performed for the  $\text{Bi}_{0.86}\text{La}_{0.14}\text{Fe}_{1-x}\text{Mn}_x\text{O}_3$  ( $x = 0.05, 0.1, 0.15$ ) samples at room temperature allowed the preliminary phase and structural analysis to be carried out. The diffraction data have confirmed the absence of any impurity phases in the materials under study. The samples with  $x = 0$  are known to possess single-phase rhombohedral structure with the  $R3c$  symmetry permitting the development of spontaneous polarization along the  $(111)_p$  directions of the parent cubic perovskite lattice (figure 1) [10, 11, 19]. The XRD pattern collected for the compound with  $x = 0.05$  has been successfully refined using a two-phase structural model suggesting the coexistence of the major ( $\sim 90\%$ ) polar rhombohedral and minor ( $\sim 10\%$ )

antipolar orthorhombic phases. The latter is largely isostructural with that of the  $\text{PbZrO}_3$  perovskite exhibiting the mutually compensative polar displacements of the A-site ions from their prototypic perovskite sites along the  $[110/\bar{1}0]_p$  directions (space group  $Pbam$ , figure 1) [19, 20]. An increase in the Mn concentration leads to a rapid increase in the fraction of the antipolar phase at the expense of the rhombohedral phase. Indeed, in the  $\text{Bi}_{0.86}\text{La}_{0.14}\text{Fe}_{0.9}\text{Mn}_{0.1}\text{O}_3$  compound, the antiferroelectric phase has been found to be dominant ( $\sim 83\%$ ). A further increase in the Mn content results in a vanishing of the  $R3c$  phase. The narrow concentration range determining the two-phase region at room temperature points at the high chemical homogeneity of the solid solutions and supports the choice of the synthesis conditions used to prepare the samples. The phase ratios calculated based on the laboratory XRD measurements have been further confirmed by the structural analysis performed using the synchrotron and neutron powder diffraction data. In particular, figure 2 shows typical results of the Rietveld refinement and illustrates the compositional evolution of the diffraction peaks reflecting the substitution-induced polar-antipolar structural phase transformation (right inset in figure 2).

The pattern of composition-driven structural changes in the  $\text{Bi}_{0.86}\text{La}_{0.14}\text{Fe}_{1-x}\text{Mn}_x\text{O}_3$  system is generally similar to that characteristic of the  $\text{Bi}_{1-x}\text{RE}_x\text{FeO}_3$  perovskites [10–13]. Both Mn and RE substitution results in decrease of the unit cell volume, suppresses the existing polar displacements (in the Mn-containing series, ionic component of the ferroelectric polarization calculated using a point charge model [21] decreases from  $\sim 63 \mu\text{C cm}^{-2}$  for  $x = 0.05$  to  $\sim 56 \mu\text{C cm}^{-2}$  for  $x = 0.1$ ) and stabilizes an antipolar state. Diminishing of the polarization followed by the FE-AFE transformation can be also observed in the pure  $\text{BiFeO}_3$  ceramics exposed to high pressure [22]. The origin of the polar-antipolar transition has been considered as related to the complex interplay of structural distortions due to the stereochemically active  $6s^2$  lone pair of the  $\text{Bi}^{3+}$  ions and rotations of  $\text{FeO}_6$  octahedra, as modified by compression [22]. This assumption is consistent with the results of our high-temperature synchrotron and



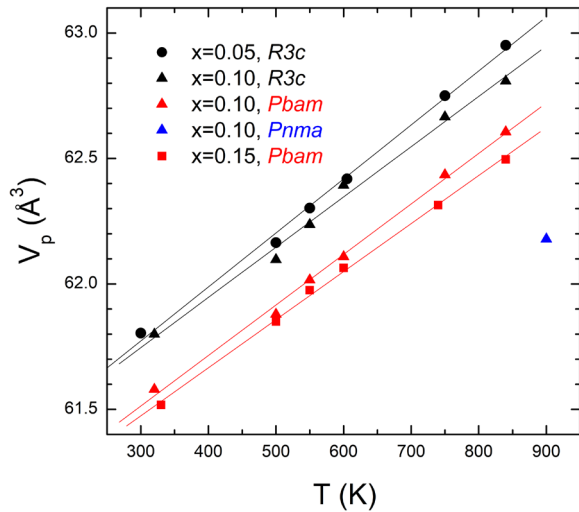


**Figure 4.** Primitive cell volume for the polar (black symbols), antipolar (red symbols) and nonpolar (blue symbols) phases of the  $\text{Bi}_{0.86}\text{La}_{0.14}\text{Fe}_{1-x}\text{Mn}_x\text{O}_3$  compounds as a function of temperature. The lines are linear fits.

neutron diffraction measurements (figures 3 and 4) indicating that the polar phase can be recovered upon thermal expansion (left inset in figure 2). A similar phenomenon has been previously observed for the  $\text{Bi}_{1-x}\text{La}_x\text{FeO}_3$  ceramics [10]. While the  $x = 0.05$  sample demonstrates a complete revival of the rhombohedral phase upon heating (left inset in figure 2), the  $x = 0.1$  compound retains a mixed structural state (with dominating ( $\sim 75\%$ ) AFE phase) up to  $T = 840$  K. An increase in the temperature up to 900 K (figure 3(b)) stabilizes the nonpolar orthorhombic  $\text{GdFeO}_3$ -type structure (space group  $Pnma$ , figure 1) which can be considered as a typical high-temperature form characteristic of bismuth ferrites [23, 24] (temperature of the heating-induced polar-nonpolar or antipolar-nonpolar transformation in the  $\text{BiFeO}_3$ -based perovskites is known to decrease with an increase in the Mn concentration) [24]. The initial structural state of the  $x = 0.05$  and  $x = 0.1$  samples recovers upon cooling back to room temperature. The  $x = 0.15$  compound maintains its monophasic AFE state over the entire temperature range under study (i.e. up to 840 K) (figure 3(c)). All the samples exhibit a linear-like increase of the primitive cell volume in the polar and antipolar phases as temperature increases (figure 4). The volumetric thermal expansion coefficients,  $\beta = \frac{1}{V} \frac{\partial V}{\partial T}$ , weakly depend on the phase composition of the materials and vary from  $3.4 \times 10^{-5} \text{ K}^{-1}$  for the  $R3c$  phase of the  $x = 0.05$  sample to  $3.1 \times 10^{-5} \text{ K}^{-1}$  for the  $Pbam$  phase of the  $x = 0.15$  sample. These values are very close to those previously reported for the polar compounds of the  $\text{Bi}_{1-x}\text{Ca}_x\text{FeO}_{3-x/2}$  multiferroics [25].

### 3.2. Magnetic properties

Magnetization measurements of the  $\text{Bi}_{0.86}\text{La}_{0.14}\text{Fe}_{1-x}\text{Mn}_x\text{O}_3$  samples suggest that Mn substitution can dramatically affect the magnetic structure of lightly-doped  $\text{Bi}_{1-x}\text{La}_x\text{FeO}_3$ . The La doping is known to reduce the threshold magnetic field required to suppress the cycloidal spin ordering characteristic

of the polar  $R3c$  phase (the reduction can be interpreted in terms of increasing anisotropy energy density taking place with increasing La content) [26]. However, a critical La concentration that would yield weak ferromagnetism at  $H = 0$  exceeds the upper limit of the compositional range for the ferroelectric phase existence ( $x \approx 0.18$ ), so a pure wFM state is realized only in antipolar (nonpolar) compounds of the  $\text{Bi}_{1-x}\text{La}_x\text{FeO}_3$  series [10, 11]. In the sample  $\text{Bi}_{0.85}\text{La}_{0.15}\text{FeO}_3$ , where the rhombohedral structure is still present, the field of 70–80 kOe for complete transition to the spin-canted (wFM) phase has been reported [26]. Despite the smaller concentration of La in the  $\text{Bi}_{0.86}\text{La}_{0.14}\text{Fe}_{0.95}\text{Mn}_{0.05}\text{O}_3$  compound, its magnetic measurements indicate that the pure wFM phase can be stabilized at the lower field of 60 kOe (figure 5(a)). Being consistent with the inhomogeneous structural state of this material, its field dependence of magnetization combines the features expected for the polar and antipolar phases. Indeed, one can see that a metamagnetic behavior (deviation from a linear increase in magnetization observed in the middle field range and associated with the reversible field-induced suppression of the cycloidal modulation in the polar phase) [26] coexists with a nonzero remanent magnetization which might be originated from the spatially-homogeneous canted magnetic arrangement specific to the antiferroelectric phase [10, 11] (figure 5(a)). Since the polar and antipolar phases are supposed to possess the same magnetization in a wFM state [10], one can determine the amount of the wFM phase at zero field. A linear extrapolation of the high field magnetization to  $H = 0$  yields  $M \approx 0.27 \text{ emu g}^{-1}$  (this magnetization would correspond to the spontaneous one if the cycloidal modulation was completely suppressed). Remanent magnetization of the sample ( $M_r \approx 0.075 \text{ emu g}^{-1}$ ) establishes the lowest limit for the content of the phase demonstrating spontaneous weak ferromagnetic behavior, thus implying that not less than 27% of the sample ( $27\% \lesssim 0.075/0.27 \times 100\%$ ) should be in a wFM state. Taking into account that the x-ray and neutron diffraction data indicate that the  $\text{Bi}_{0.86}\text{La}_{0.14}\text{Fe}_{0.95}\text{Mn}_{0.05}\text{O}_3$  sample contains only around 10% of the antipolar phase, one can suppose that the polar  $R3c$  phase also contributes to the resulting net magnetization. This assumption is further confirmed by the magnetic data obtained for the  $x = 0.1$  and  $x = 0.15$  compounds (figures 5(b) and (c)). The former, containing about 17% of the polar phase at room temperature, possesses spontaneous magnetization ( $M_s \approx 0.225 \text{ emu g}^{-1}$ ) exceeding that observed for the purely antipolar sample ( $M_s \approx 0.185 \text{ emu g}^{-1}$ ). Accordingly, our investigation indicates that the Mn substitution affects the stability of the cycloidal order in the ferroelectric phase of the  $\text{Bi}_{1-x}\text{La}_x\text{FeO}_3$  multiferroics and induces the antiferromagnetic  $\rightarrow$  weak ferromagnetic transformation. This conclusion is consistent with the previous studies reporting on the observation of a Mn doping-stabilized weak ferromagnetic/ferroelectric phase appearing in the  $\text{Bi}_{1-x}\text{Pr}_x\text{FeO}_3$  [27] and  $\text{Bi}_{1-x}\text{Nd}_x\text{FeO}_3$  [15] series near the polar-antipolar phase boundary. A decrease in the spontaneous (or magnetic-field stabilized) room-temperature magnetization taking place in the  $\text{Bi}_{0.86}\text{La}_{0.14}\text{Fe}_{1-x}\text{Mn}_x\text{O}_3$  system with an increase in the Mn concentration (figure 5) correlates with the

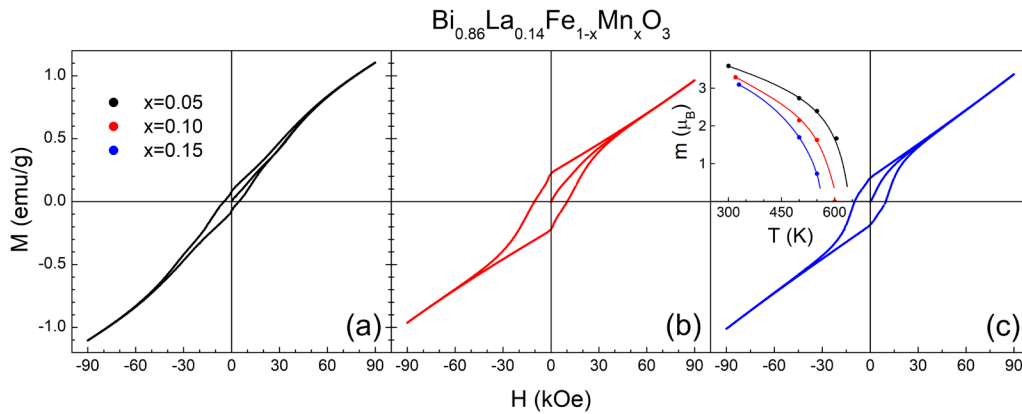


**Figure 5.** Magnetic hysteresis loops obtained for the  $\text{Bi}_{0.86}\text{La}_{0.14}\text{Fe}_{1-x}\text{Mn}_x\text{O}_3$  samples at room temperature. The inset demonstrates the temperature evolution of the ordered magnetic moment per Fe/Mn as determined from the Rietveld refinement of NPD data (since the magnetic satellite peaks associated with the cycloidal spin modulation in the  $R3c$  phase cannot be observed because of the resolution limitations of the instrument at long  $d$ -spacings, the simplified model [25] assuming an antiferromagnetic  $G$ -type ordering of the magnetic moments aligned along the hexagonal  $a$  axis was applied; the refinement further suggests that the  $Pbam$  phase is characterized by a  $G$ -type AFM order and the magnetic moments are oriented along the  $c$  axis). The lines are guides for the eye. Black, red, and blue symbols are used for the samples with  $x = 0.05, 0.01, \text{ and } 0.15$ , respectively.

NPD data (inset in figure 5(c)) which suggest the lowering of the Neel temperature with increasing  $x$ , as expected from the corresponding change in the average number of  $e_g$  electrons on the  $B$  site [28]. The pattern of composition- and temperature-driven evolution of the ordered magnetic moment in the  $\text{Bi}_{0.86}\text{La}_{0.14}\text{Fe}_{1-x}\text{Mn}_x\text{O}_3$  series (inset in figure 5(c)) is consistent with the previous NPD data obtained for the Mn-doped  $\text{BiFeO}_3$ -based perovskites [29, 30].

It is interesting to note that, when taken alone, neither Mn nor rare-earth doping can be effectively used to obtain the pure wFM state in the polar phase [28, 31–34]. The combined substitution, in contrast, seems to be able to ensure a delicate balance between the structural and magnetic instabilities, thus providing an unusual possibility to achieve the switchable magnetization and ferroelectric polarization in the same phase. The nature of the chemical pressure-induced suppression of the cycloidal ordering in the polar phase of  $\text{BiFeO}_3$ -based multiferroics can be generally understood in terms of composition-driven changes in the polarization-related and oxygen octahedra rotation-related components of the Dzyaloshinskii–Moriya (DM) interaction [35]. It is supposed that if the DM energy associated with the ferroelectric polarization becomes smaller than that of the octahedral rotations, the cycloidal state is destabilized in favour of a  $G$ -type structure with a net ferromagnetic component induced by spin canting in the basal plane [35]. Since our current and previously reported [15, 28, 29] structural data indicate that Mn substitution suppresses the existing polar ionic displacements in bismuth ferrites (even though it does not necessarily indicate that measured ferroelectric polarization will always decrease with increasing Mn content—Mn doping can influence the leakage current density, thus affecting the macroscopic measurements [36]), the reasons underlying the cycloidal magnetic structure versus canted magnetic structure instability in the rhombohedral phase of the  $\text{Bi}_{0.86}\text{La}_{0.14}\text{Fe}_{1-x}\text{Mn}_x\text{O}_3$  perovskites can be interpreted as having magnetoelectric origin (removal of the cycloidal magnetic modulation via the doping-driven reduction of the ferroelectric polarization) [37].

## 4. Conclusions

Synchrotron x-ray and neutron powder diffraction measurements of the  $\text{Bi}_{0.86}\text{La}_{0.14}\text{Fe}_{1-x}\text{Mn}_x\text{O}_3$  ( $x = 0.05, 0.1, 0.15$ ) samples have been performed over a wide (from 300 K to 900 K) temperature range to disclose how Mn substitution influences structural stability of the  $\text{Bi}_{1-x}\text{La}_x\text{FeO}_3$  multiferroics near their polar-antipolar (rhombohedral-orthorhombic) phase boundary. It has been proven that the substitution tends to suppress the existing polar displacements and stabilizes the antiferroelectric  $\text{PbZrO}_3$ -like structure. The polar and antipolar phases coexist at  $0.05 \leq x \leq 0.1$ . Depending on the initial phase composition at room temperature, the ferroelectric phase can be either fully or partly recovered by heating. The heating-induced transformation is not irreversible. Magnetic measurements supplemented the results of the diffraction study indicate that the combined substitution affects the stability of the cycloidal antiferromagnetic order in the polar phase and a mixed La/Mn doping of  $\text{BiFeO}_3$  could be therefore considered as a promising future strategy to attain spontaneous magnetization and polarization in a structurally-homogeneous, single-phase material.

## Acknowledgments

This work has received funding from the European Union’s Horizon 2020 research and innovation programme under the Marie Skłodowska-Curie grant agreement No 778070. The work was also supported by funds from FEDER (Programa Operacional Factores de Competitividade—COMPETE) and FCT—Fundação para a Ciência e a Tecnologia (project UID/FIS/04564/2016). V A K is grateful to Fundação para a Ciência e a Tecnologia for financial support through the FCT Investigator Programme (project IF/00819/2014/CP1223/CT0011). M S I is grateful to FCT for financial support through the project MATIS—Materiais e Tecnologias Industriais Sustentáveis (CENTRO-01-0145-FEDER-000014). M

V S and D V K acknowledge RFBR (#17-58-45026 IND\_a), R R acknowledges DST (INT/RUS/RFBR/P-299). Access to TAIL-UC facility funded under QREN-Mais Centro project ICT\_2009\_02\_012\_1890 is gratefully acknowledged as well.

## ORCID iDs

V A Khomchenko  <https://orcid.org/0000-0002-5867-3297>

M S Ivanov  <https://orcid.org/0000-0001-9155-9288>

## References

- [1] Vopson M M 2015 *Crit. Rev. Solid State Mater. Sci.* **40** 223
- [2] Hu J-M, Chen L-Q and Nan C-W 2016 *Adv. Mater.* **28** 15
- [3] Catalan G and Scott J F 2009 *Adv. Mater.* **21** 2463
- [4] Wu J, Fan Z, Xiao D, Zhu J and Wang J 2016 *Prog. Mater. Sci.* **84** 335
- [5] Kubel F and Schmid H 1990 *Acta Cryst. B* **46** 698
- [6] Johnson R D, Barone P, Bombardi A, Bean R J, Picozzi S, Radaelli P G, Oh Y S, Cheong S-W and Chapon L C 2013 *Phys. Rev. Lett.* **110** 217206
- [7] Kadomtseva A M, Popov Yu F, Pyatakov A P, Vorob'ev G P, Zvezdin A K and Viehland D 2006 *Phase Transit.* **79** 1019
- [8] Tabares-Munoz C, Rivera J-P, Bezinges A, Monnier A and Schmid H 1985 *Japan. J. Appl. Phys.* **24** 1051
- [9] Yang Y, Infante I C, Dkhil B and Bellaiche L 2015 *C. R. Phys.* **16** 193
- [10] Troyanchuk I O, Karpinsky D V, Bushinsky M V, Khomchenko V A, Kakazei G N, Araujo J P, Tovar M, Sikolenko V, Efimov V and Kholkin A L 2011 *Phys. Rev. B* **83** 054109
- [11] Rusakov D A, Abakumov A M, Yamaura K, Belik A A, Van Tendeloo G and Takayama-Muromachi E 2011 *Chem. Mater.* **23** 285
- [12] Khomchenko V A, Troyanchuk I O, Bushinsky M V, Mantyskaya O S, Sikolenko V and Paixão J A 2011 *Mater. Lett.* **65** 1970
- [13] Troyanchuk I O, Karpinsky D V, Bushinsky M V, Mantyskaya O S, Tereshko N V and Shut V N 2011 *J. Am. Ceram. Soc.* **94** 4502
- [14] Khomchenko V A, Ivanov M S, Karpinsky D V and Paixão J A 2017 *J. Appl. Phys.* **122** 124103
- [15] Khomchenko V A, Karpinsky D V, Pereira L C J, Kholkin A L and Paixão J A 2013 *J. Appl. Phys.* **113** 214112
- [16] Walker J et al 2016 *Sci. Rep.* **6** 19630
- [17] Liao Z, Xue F, Sun W, Song D, Zhang Q, Li J-F, Chen L-Q and Zhu J 2017 *Phys. Rev. B* **95** 214101
- [18] Rodríguez-Carvajal J 1993 *Physica B* **192** 55
- [19] Khomchenko V A, Troyanchuk I O, Karpinsky D V, Das S, Amaral V S, Tovar M, Sikolenko V and Paixão J A 2012 *J. Appl. Phys.* **112** 084102
- [20] Glazer A M, Roleder K and Dec J 1993 *Acta Cryst. B* **49** 846
- [21] Avdeev M, Jorgensen J D, Short S, Samara G A, Venturini E L, Yang P and Morosin B 2006 *Phys. Rev. B* **73** 064105
- [22] Kozlenko D P, Belik A A, Belushkin A V, Lukin E V, Marshall W G, Savenko B N and Takayama-Muromachi E 2011 *Phys. Rev. B* **84** 094108
- [23] Arnold D C, Knight K S, Morrison F D and Lightfoot P 2009 *Phys. Rev. Lett.* **102** 027602
- [24] Khomchenko V A, Troyanchuk I O, Maria T M R, Karpinsky D V, Das S, Amaral V S and Paixão J A 2012 *J. Appl. Phys.* **112** 064105
- [25] Khomchenko V A, Troyanchuk I O, Többsens D M, Sikolenko V and Paixão J A 2013 *J. Phys.: Condens. Matter* **25** 135902
- [26] Le Bras G, Colson D, Forget A, Genand-Riondet N, Tourbot R and Bonville P 2009 *Phys. Rev. B* **80** 134417
- [27] Khomchenko V A, Troyanchuk I O, Kovetskaya M I, Kopcewicz M and Paixão J A 2012 *J. Phys. D: Appl. Phys.* **45** 045302
- [28] Selbach S M, Tybell T, Einarsrud M-A and Grande T 2009 *Chem. Mater.* **21** 5176
- [29] Sosnowska I, Schäfer W, Kockelmann W, Andersen K H and Troyanchuk I O 2002 *Appl. Phys. A* **74** S1040
- [30] Saxin S and Knee C S 2011 *Dalton Trans.* **40** 3462
- [31] Belik A A, Abakumov A M, Tsirlin A A, Hadermann J, Kim J, Van Tendeloo G and Takayama-Muromachi E 2011 *Chem. Mater.* **23** 4505
- [32] Khomchenko V A, Pereira L C J and Paixão J A 2011 *J. Phys. D: Appl. Phys.* **44** 185406
- [33] Khomchenko V A, Troyanchuk I O, Karpinsky D V and Paixão J A 2012 *J. Mater. Sci.* **47** 1578
- [34] Bielecki J, Svedlindh P, Tibebu D T, Cai S, Eriksson S-G, Börjesson L and Knee C S 2012 *Phys. Rev. B* **86** 184422
- [35] Johnson R D, McClarty P A, Khalyavin D D, Manuel P, Svedlindh P and Knee C S 2017 *Phys. Rev. B* **95** 054420
- [36] Singh S K, Ishiwara H and Maruyama K 2006 *Appl. Phys. Lett.* **88** 262908
- [37] Khomchenko V A, Karpinsky D V and Paixão J A 2017 *J. Mater. Chem. C* **5** 3623